

High-speed holographic optical tweezers using a ferroelectric liquid crystal microdisplay

William J Hossack, Eirini Theofanidou and Jason Crain

*School of Physics, The University of Edinburgh, King's Buildings, Mayfield Road, Edinburgh
EH9 3JZ, Scotland*

w.hossack@ed.ac.uk

<http://www.ph.ed.ac.uk>

Kevin Heggarty

Dept Optique, ENST de Bretagne, BP 832, 29285 Brest cedex, France

Martin Birch

CRL Opto Limited, 1 St David's Drive, Dalgety Bay, Dunfermline, KY11 9PF, Scotland

Abstract: We demonstrate the advantages of a ferroelectric liquid crystal spatial light modulator for optical tweezer array applications. The fast switching speeds of the ferroelectric device (compared to conventional nematic systems) is shown to enable very rapid reconfiguration of trap geometries, controlled, high speed particle movement, and tweezer array multiplexing.

© 2003 Optical Society of America

OCIS codes: (140.0140) Lasers and laser optics; (140.7010) Trapping; (120.0120) Instrumentation, measurement and methodology; (180.0180) Microscopy; (090.0090) Holography; (090.1970) Diffractive Optics; (230.0230) Optical Devices; (230.6120) Spatial Light Modulators

References and links

1. A. Ashkin, J. M. Dziedzic, J. E. Bjorkholm and S. Chu, "Observation of a single beam gradient force optical trap for dielectric particles," *Opt. Lett.* **11**, 288, (1986)
2. K. Dholakia, G. Spalding and M. MacDonald, "Optical tweezers: the next generation," *Physics World* **15-10** (October 2002)
3. P.T. Korda, G.C. Spalding and D.G. Greir, "Evolution of a colloidal critical state in an optical pinning potential landscape", *Phys. Rev. B* **66**, 024504 (2002)
4. R.L. Eriksen, V.R. Daria, P.J. Rodrigo, J. Gluckstad, "Computer controlled orientation of multiple optically-trapped particles," *Microelectronic Engineering* **67-68**, 872, (2003)
5. S. M. Block, H. C. Blair and H. C. Berg, "Compliance of bacterial flagella measured with optical tweezers," *Nature (London)* **338**, 514, (1989)
6. M. D. Wang, H. Yin, R. Landick, J. Gelles and S. M. Block, "Stretching DNA with optical tweezers," *Biophysics J.* **72**, 1335 (1997)
7. W.M. Lee, X.C. Yuan and D. Y. Tang, "Optical tweezers with multiple optical forces using double-hologram interference," *Opt. Express* **11**, 199, (2003)
8. P.J. Rodrigo, R. L. Eriksen, V.R. Daria and J. Glueckstad, "Shack-Hartmann multiple-beam optical tweezers," *Opt. Express* **11**, 208, (2003)
9. H. Dammann and K. Gortler, "High-efficiency in-line multiple imaging by means of multiple phase holograms," *Opt. Commun.* **3** 312 (1971)
10. M.P. Dames, R.J. Dowling, P. McKee and D. Wood, "Efficient optical elements to generate intensity weighted spot arrays: design and fabrication," *Appl. Opt.* **30** 2685 (1991)
11. N.R Heckenburg, R. McDuff, C.P. Smith, H. Rubinsztein-Dunlop, and M.J. Wegener, "Laser beams with phase singularities," *Opt. Quantum Electron.* **24**, S951 (1992)

12. C. D'Helon, E.W. Dearden, H. Rubinsztein-Dunlop and N.R. Heckenburg, "Measurement of the Optical Force and Trapping Range of a Single-beam Gradient Optical Trap for Micron-sized Latex Spheres," *J. Mod. Opt.* **41**, 595, (1994)
 13. E.R. Dufresne and D.G. Grier, "Optical tweezer arrays and optical substrates created with diffractive optics," *Rev. Sci. Inst.* **69**, 1974, (1998)
 14. E.R. Dufresne, G.C. Spalding, M.T. Dearing, S.A. Sheets and D.G. Grier "Computer-generated holographic optical tweezer arrays," *Rev. Sci. Inst.* **72**, 1810, (2002)
 15. Hamamatsu Photonics, <http://www.hamamatsu.com>
 16. CRL Opto Ltd, <http://www.crlopto.com>
 17. K.M Johnson, M.A. Handschy and L.A. Pagano-Stauffer "Optical computing and image processing with ferroelectric liquid crystals," *Opt. Eng.* **16**, 385 (1987)
 18. J.E. Curtis, B.A. Kes and D.G. Grier, "Dynamic holographic optical tweezers," *Opt. Commun.* **207**, 169, (2002)
-

1. Introduction

Since the principle of optical trapping was demonstrated in the 1980's [1], laser tweezers have emerged as a powerful micromanipulation tool in both the physical and life sciences. Over this period, it has been recognised that the functionality of a single-gradient optical tweezer can be extended significantly by engineering multiple steerable traps [2]. These optical tweezer arrays bring major potential advantages for aspects of colloidal science [3], cell biology [4] and single molecule biophysics [5, 6].

The most powerful and versatile approach for creating complex trapping landscapes involves the use of dynamic diffractive optical elements. Here, steering and manipulation is realised by encoding holographic patterns onto a reconfigurable device [2, 7, 8]. The method relies on computer-generated phase-only holographic patterns for optical fan-out which date back to Dammann [9] and have been extended to two-dimensional formulations by Dames [10]. Holographic elements for optical tweezers and beam shaping were first implemented by Heckenberg [11, 12] to form Laguerre Gaussian beams, and by Grier et al, for multiple tweezers, initially with fixed holograms [13], and subsequently using dynamic holograms [14].

To our knowledge, nearly all reported dynamic holographic laser tweezer applications have used spatial light modulators (SLMs) based on *nematic* liquid crystals; the most common being the *Programmable Phase Modulator* from Hamamatsu [15]. These have been used by several authors as described in the review by Dholokia [2] and references therein. However, the re-configuration speed of these devices is strictly limited by the relatively slow switching times (tens of milliseconds) characteristic of nematic liquid crystals. The resulting speed v of particle movement (imposed by device response time) is therefore restricted to regimes far slower than the "ultimate" speed limit which is not reached until the Stokes drag force ($F_D = 6\pi\eta Rv$) becomes comparable to the trap strength (of order 10 piconewtons). Here η is the viscosity of the medium, R is the particle radius. As a result, the opportunities in optical tweezer technology that may be created by faster switching devices have been largely unexplored.

Unlike nematic materials, *ferroelectric* liquid crystal molecules form low-symmetry chiral phases which support a net spontaneous polarisation that couples linearly to applied electric fields. As a result, SLM's based on ferroelectric materials show extremely fast ($< 100\mu\text{s}$) switching. This is nearly two orders of magnitude faster than conventional nematic devices. The advantages of this ultrafast response time for optical trapping applications is explored in the present paper.

Specifically, we demonstrate the operation of a holographic trap array system based on a ferroelectric liquid crystal light modulator. We focus on those applications of optical trap arrays than may benefit most directly from the large increase in switching speed afforded by ferroelectric liquid crystal technology. In particular, we demonstrate rapid reconfiguration of the trap landscape, high speed particle movement up to $35\mu\text{m s}^{-1}$, (approaching the practical limit imposed by viscous drag) and trap multiplexing which we demonstrate as an efficient method

of populating traps of complex geometries.

2. Ferroelectric liquid crystal microdisplays for laser tweezer applications

For the diffractive element in the optical tweezer system we use the CRL Opto SXGA1-R2-H1 microdisplay [16]. This is a 1280×1024 reflective pixel array on a $13.62\mu\text{m}$ pitch switching a ferroelectric liquid crystal modulator layer. The commercial display version of this device is designed for visible light display applications with a 33° switching angle for green light. For optimal use as a reconfigurable diffractive device, pure-binary phase modulation is preferable requiring a switching angle of 90° . Such devices are currently under development at CRL Opto with diffraction efficiencies of 25% being obtained in each useful order. The results presented here however, were obtained using the commercial display (33° switching angle) with a correspondingly reduced optical throughput. For use as a binary phase modulator the device is placed between crossed polarisers with the the incident polarisation aligned to half the cone switching angle giving an absolute phase shift of π between pixels in the two switched states [17]. By Babinet's principal, for diffractive applications the positive and negative DC balanced frames are identical. Due to the binary phase operation of ferroelectric devices, the arrangement of tweezer traps must always form a centro-symmetric pattern.

As ferroelectric device displays only binary images, for display applications, colour images are built up by colour sequential temporal multiplexing synchronised with the light sources. The device is driven from a PC through a Digital Video Interface (DVI) with 24 bit colour images at 60 Hz. For our purposes this means 24 different bit-planes are available in each 60Hz time slot giving a binary image refresh rate of 1440 Hz. To use effectively such high refresh rates the diffraction patterns must be sent to the device at comparable rates. We have used two techniques to take advantage of the ferroelectric liquid crystal speed in optical tweezer applications.

1. *Non-Multiplexed Hologram*. The same binary pattern is in all 24 bit planes:
 - (a) The patterns are a series of pre-calculated images stored in PC memory and flashed out to the SLM through the video link. The refresh rate is PC dependent but rates of > 10 images/s are generally achieved on a standard PC.
 - (b) For some diffractive patterns which can be described as vector structures (gratings, diffractive lenses, Dammann gratings) the patterns can be drawn as vector patterns and manipulated (rotated, shifted, scaled causing the trap position to move accordingly) using the hardware accelerated video routines of the video card. With this technique rates of > 30 images/s have been obtained making real time control of trap position possible
2. *Multiplexed Holograms*: Different diffractive patterns can be loaded into the different bit-planes which are then displayed in order by the microdisplay interface. This allows 24 different holograms to be displayed sequentially within one 60Hz video frame. Due to the high update speed the optical laser power is shared equally between the 24 holograms. Again, the whole pattern can be updated as for the *non-multiplexed hologram* mode, allowing a highly flexible dynamically programmable diffractive device.

The system control software runs under Linux/KDE on a standard PC with a Matrox G550 dual-head video card enabling the diffracting pattern data to be sent to the SLM video port and controlled from a user interface on the monitor port. The software uses *OpenGL* routines to access the video hardware acceleration.

3. Optical system

A schematic of the optical system is shown in Fig. 1. Collimated output from a red Kr⁺-ion or He-Ne laser is expanded to illuminate a circular area of the microdisplay approximately 1000 pixels (11mm) in diameter. The polarising beam splitter acts as the analyser giving pure binary phase modulation. The 250 mm and 120 mm lens pair form a 4-f imaging system that project

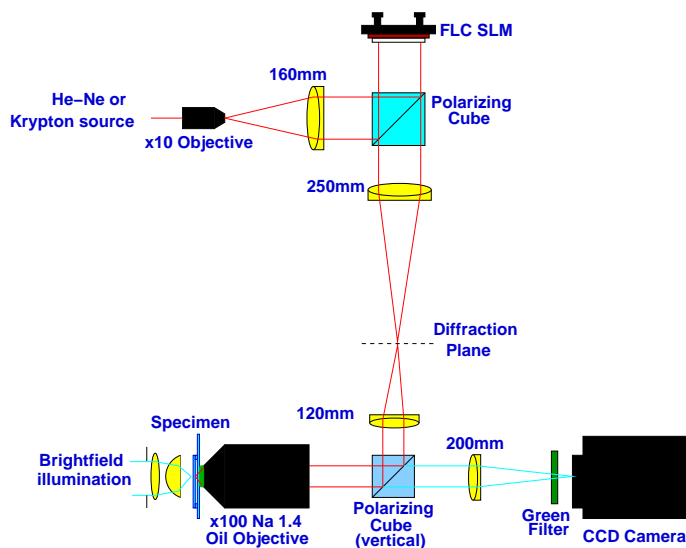


Fig. 1. Schematic layout of optical system

an image, into the back aperture of the microscope objective scaled in size by 0.48 via a second polarised beam splitter oriented to transmit 100% of the tweezer illumination. The microscope objective is a Nikon $\times 100$, 1.4 NA, oil objective with a back exit pupil of 6.5 mm with bright field imaging to a video camera giving a field of view of $40 \times 60 \mu\text{m}$. The whole system is incorporated in an inverted microscope geometry as detailed in Fig. 1.

With this optical layout, a binary grating on the input microdisplay of 12 pixels pitch results in first order diffraction spots at $\pm 20.8 \mu\text{m}$ using He-Ne illumination; the full field of view of the objective.

4. Non-multiplexed hologram results

All trapping experiments take place with $1 \mu\text{m}$ polystyrene spheres suspended in distilled water.

In Fig. 2 we show a 4-by-4 tweezer array on a $5 \mu\text{m}$ pitch. The holographic pattern was calculated using the iterative techniques proposed by Dames[10] in which a 128×128 pixel pattern is replicated across the microdisplay. Initial trapping of the spheres was achieved using a Kr⁺ laser power of 700 mW. All traps were then be maintained at a reduced power of 300 mW. This gives an estimated input requirement of approximately 43 mW per trap.

Based on these static experiments, and keeping within the 4W incident power damage limit of the device, we estimate that a maximum of approximately 90 usable traps could be created with the commercial display oriented device. This figure rises to several hundred with the binary-phase-optimised device under development. This is comparable with results obtained from nematic devices.

Movable traps were implemented by writing binary gratings described as *OpenGL* vector



Fig. 2. (0.6 MB) Movie of 4×4 array of traps on $5 \mu\text{m}$ pitch with 700 mW total input power showing capture of final trap.

objects. This permitted real-time scaling and rotation of the pattern using the built-in graphics acceleration hardware. Strong traps were formed with approximately 50 mW input power per trap from the Krypton laser. Motion was obtained by scaling or rotating the gratings to move the trap. Results are shown in Fig. 3 and in associated linked movies.



Fig. 3. (1.5 MB) Movie of two movable array of traps rotating two beads in a $10.5 \mu\text{m}$ circle with maximum speed of $35 \mu\text{ms}^{-1}$.

The maximum speed obtained for stable traps with the current graphics hardware was $35 \mu\text{ms}^{-1}$ while rotating two traps in a $10.5 \mu\text{m}$ diameter circle by rotation the grating in 12° steps using 700 mW of laser power which corresponds to approximately 32 scaled frame per with approximately $1.1 \mu\text{m}$ between successive traps. Higher speeds, implemented by increasing the angle step and thus separation between successive traps, resulted in loss of beads. It is unclear from initial experiments if this loss results from the Stokes drag limit or excessive separation between the successive traps.

The video hardware is operating at half the operation speed of the the microdisplay which operates at 60 Hz, so giving the system a potential trap movement speed in excess of $66 \mu\text{ms}^{-1}$ with the current step size. Using a nematic device the maximum demonstrated trap movement speed is $2.5 \mu\text{ms}^{-1}$ [4] and the maximum proposed is $10 \mu\text{ms}^{-1}$ [18].

5. Multiplexed holographic trap geometries

The most powerful feature of holographic optical traps based on ferroelectric devices is the possibility of multiplexing trap landscapes to enhance flexibility and functionality of the arrays. Here the fast-switching property of the ferroelectric device is deployed not only to move particles rapidly but to time-share between geometries. Here we illustrate the operation by partitioning the output of the 24 bitplane device to create a multiplexed configuration comprising independent static and dynamic arrays.

Specifically, a linear 5×1 static array of traps was formed by using 16 of the 24 bitplanes (denoted as the “red” and “green” channels) and two movable traps by the remaining 8 bitplanes (“blue” channel). This results in the composite hologram illustrated in Fig. 4 which shows a

“yellow” vertical grating to generate the 5×1 array, overlaid with the “blue” grating at 45° which generates the two movable traps. The optical trapping results are shown in Fig. 5 and its associated linked movie.

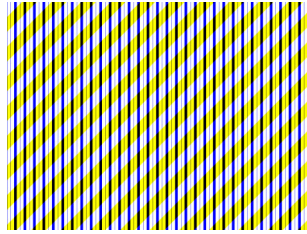


Fig. 4. Composite hologram for 5×1 static hologram in “red” and “green” channels and two trap hologram in “blue” channel.

This resulted in a one-third to two-thirds time multiplexed split of the diffracted output. The fast-switching of the device is crucial for robust operation because the timescale over which the multiplexing leaves a particle unilluminated must be short compared to the particle’s diffusion time, which is typically many 10s of milliseconds.

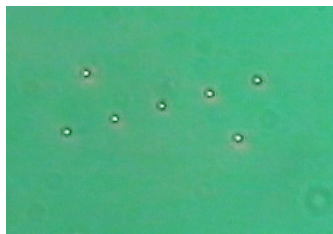


Fig. 5. (2.46 MB) Movie showing five fixed and two movable traps formed by two-to-one multiplex.

Due to the complex structure of the multiplexed hologram the full 24 bit images is currently calculated by using the control computer without the advantage of *OpenGL* acceleration. The required holograms were generated in real-time from a pre-calculated 5×1 fan-out hologram formed by the Dames [10] technique overlaid by a dynamically calculated grating with pitch and orientation controlled from an X-windows control panel. This resulted in an update rate of 3 images per second with the current 1.4 GHz PC. We believe that with faster computer / graphics hardware and optimised coding image rates of 10 images per second will be obtainable. This will be faster if the bit-level image is formed using *OpenGL* acceleration. The ultimate limit is 60 images per second determined by the microdisplay frame display rate.

Using the previous power budget of approximately 40 mW input per trap and the 4 W device damage threshold, a 4-trap dynamic hologram can be formed from each of the 24 bit-planes allowing complex dynamic patterns of up to 96 traps. A powerful application of this mode is in filling the fixed traps since the movable traps can be used to “collect” beads and move then close to the fixed trap. The movable trap can then be blanked, so allowing the bead to fall into the fixed trap array. In particular with 4 W laser illumination, 23 of the bit planes can be used for the fixed array containing up to 90 traps, and the remaining one bit-plane used to form two strong movable traps. This mode is essential for filling large fixed arrays which otherwise is a very time consuming and delicate operation.

6. Conclusions

In conclusion we have demonstrated the potential advantages of a ferroelectric liquid crystal light modulator relative to a conventional nematic device for optical trap array applications. In addition to the direct increase in trap reconfiguration speed, we also demonstrate the first multiplexed holographic trap geometries consisting of combinations of static and dynamic arrays.

Acknowledgements

We are grateful to the Royal Society for support through the Paul Instrument Fund, the COSMIC Research Centre at The University of Edinburgh and Nikon UK. We also acknowledge the Graphics and Multimedia Workshop, The University of Edinburgh for assistance in preparation of video clips.